

Microwave assisted synthesis, cholinesterase enzymes inhibitory activities and molecular docking studies of new pyridopyrimidine derivatives



Alireza Basiri^a, Vikneswaran Murugaiyah^{a,*}, Hasnah Osman^b, Raju Suresh Kumar^{c,*}, Yalda Kia^b, Mohamed Ashraf Ali^d

^a School of Pharmaceutical Sciences, Universiti Sains Malaysia, Minden 11800, Penang, Malaysia

^b School of Chemical Sciences, Universiti Sains Malaysia, Minden 11800, Penang, Malaysia

^c Department of Chemistry, College of Sciences, King Saud University, PO Box 2455, Riyadh, Saudi Arabia

^d Institute for Research in Molecular Medicine, Universiti Sains Malaysia, Minden 11800, Penang, Malaysia

ARTICLE INFO

Article history:

Received 20 February 2013

Revised 19 March 2013

Accepted 21 March 2013

Available online 1 April 2013

Keywords:

Microwave assisted synthesis

Pyridopyrimidines

AChE and BChE activity

Molecular docking

ABSTRACT

A series of hitherto unreported pyrido-pyrimidine-2-ones/pyrimidine-2-thiones were synthesized under microwave assisted solvent free reaction conditions in excellent yields and evaluated *in vitro* for their acetylcholinesterase (AChE) and butyrylcholinesterase (BChE) enzymes inhibitory activity. Among the pyridopyrimidine derivatives, **7e** and **7l** displayed 2.5- and 1.5-fold higher enzyme inhibitory activities against AChE as compared to standard drug, galanthamine, with IC_{50} of 0.80 and 1.37 μ M, respectively. Interestingly, all the compounds except **6k**, **7j** and **7k** displayed higher inhibitory potential against BChE enzyme in comparison to standard with IC_{50} ranging from 1.18 to 18.90 μ M. Molecular modeling simulations of **7e** and **7l** was performed using three-dimensional structure of *Torpedo californica* AChE (TcAChE) and human butyrylcholinesterase (hBChE) enzymes to disclose binding interaction and orientation of these molecule into the active site gorge of respective receptors.

© 2013 Elsevier Ltd. All rights reserved.

1. Introduction

According to the World Alzheimer report 2012, Alzheimer's disease (AD) is among the most significant social, health and economical crisis of the 21st century.¹ AD is a complex disease characterized by accumulation of β -amyloid ($A\beta$) plaques and neurofibrillary tangles composed of tau amyloid fibrils, associated with synapses loss and neuro-degeneration leading to impairment of memory and other cognitive dysfunctions.² The cognitive deficit is thought to be due to loss of cholinergic neurons in basal forebrain.³ One of the pharmacological approaches to restore cholinergic function is by blocking the breakdown of neurotransmitter in the cholinergic neurons, acetylcholine (ACh), leading to the use of cholinesterase inhibitors to treat AD.⁴

Acetylcholinesterase (AChE) and butyrylcholinesterase (BChE) enzymes are involved in the breakdown of acetylcholine in the brain and inhibition of these enzymes may increase the efficacy of treatment and broaden the indications.⁵ Effects of cholinesterase inhibitors are mainly due to enhancement of cholinergic transmission at cholinergic autonomic synapses and at the neuromuscular

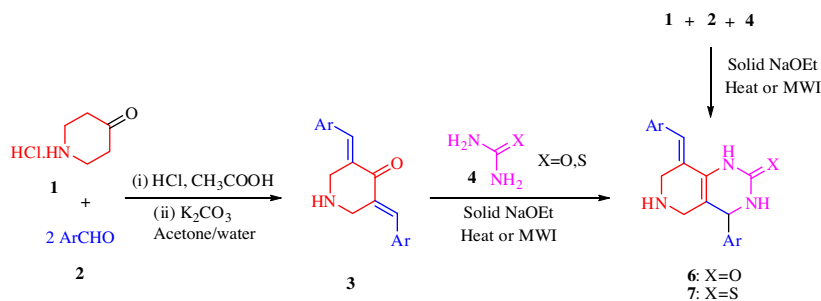
junction.⁶ Commercially available drugs such as galanthamine, donepezil, rivastigmine and tacrine showed positive results in symptomatic improvements of mild to moderate AD patients.⁷ Donepezil and galanthamine being most selective for AChE while rivastigmine inhibit AChE and BChE at the same extent and tacrine shows lower selectivity for AChE than BChE.⁸

The recent development of inhibitors includes drugs with high selectivity for BChE, which also showed enhancement of ACh levels in rats brain.⁹ BChE inhibitors were also found to reduce amyloid precursor protein levels in animals with a cholinergic lesion in the forebrain.¹⁰ These agents represent an additional advantage for long-term stabilization of cognitive and behavioral symptoms in patients with advanced AD.¹¹ A selective BChE inhibitor, may produce significant increase in brain ACh levels without triggering severe peripheral or central cholinergic adverse effects.⁸

Molecular modeling plays an important role in the rational drug design and is used to predict the bonding affinity, spatial orientation and total binding energy of the small molecule drug candidates to the active site of their target enzymes.¹² AChE's active site is located on the bottom of a long and narrow gorge, acetylcholine and substrate guidance down the gorge is facilitated by cation- π interactions with aromatic side-chains residues such as phenylalanine, tryptophan and tyrosine lining gorge wall.¹³ The overall structure of human BChE is very similar to that of AChE

* Corresponding authors. Tel./fax: +60 46534583.

E-mail addresses: vicky@usm.my (V. Murugaiyah), sraju@ksu.edu.sa (R.S. Kumar).



Scheme 1. Synthesis of 6a–I and 7a–I.

from *Torpedo California*. Most differences between BChE and TcAChE are confined to the residues composing the gorge, whereby in BChE it is replaced with hydrophobic Leu286 and Val288. These changes make it possible for the binding of bulkier butyrate substrate moiety and inhibitors in BChE.¹⁴

Natural and synthetic biologically active compounds with pyrimidinone moiety, find applications in pharmaceutical and biochemical fields¹⁵ as antihypertensive,¹⁶ α_{1a} -adrenergic receptor antagonists,¹⁷ antibacterial, anti-inflammatory and antitumor agents.¹⁸ Compounds which constitute the core structural elements of pyrimidinone are commonly present in the polycyclic marine alkaloids which show anti cancer, anti HIV and cytotoxic properties.^{19–21} Inspired by the aforementioned significance of pyrimidinone derivatives, in the present study two series of pyrimidinone derivatives were synthesized and their cholinesterase inhibitory activities were explored. Further molecular modeling was performed on the most active compounds to understand the possible reasons for their selectivity.

2. Results and discussion

2.1. Chemistry

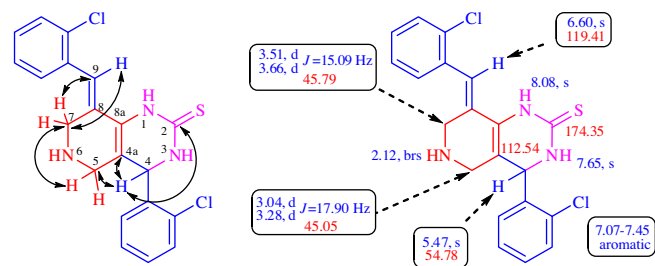
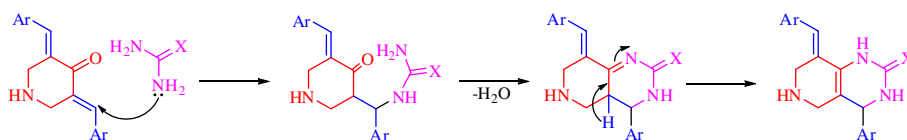
In the present investigation, the reaction of a series of N-unsubstituted dibenzylidenepiperidine-4-ones with urea/thiourea in presence of catalytic amount of solid sodium ethoxide afforded the functionalized hitherto unreported pyridopyrimidine-2-ones (6)/pyridopyrimidine-2-thiones (7) in excellent yields (Scheme 1). The N-unsubstituted dibenzylidenepiperidine-4-ones (3) required for the present study was synthesized following the literature reported method by Dimmock et al.²²

In order to find the optimal, efficient, eco-friendly and handy protocol for the synthesis of pyridopyrimidine derivatives, the reaction was examined under different conditions by choosing the model reaction between an equimolar ratio of 3,5-bis(4-methylbenzylidene)piperidin-4-one and thiourea in the presence of catalytic amount of solid sodium ethoxide. Initially, the neat reaction mixture in a semi micro boiling tube was heated in a water bath, for about 4–5 min during which period a transparent viscous liquid formed showing completion of reaction and double examined by TLC. Water (50 mL) was added to the mixture, precipitated solid

was filtered and dried in vacuo to afford the pyridopyrimidine-2-thiones (7c) in 72% yield (Method A). The product obtained by this method doesn't require further purification as it is evident from TLC and ¹H NMR spectra. The same reaction was conducted under microwave irradiation condition (Method B), as this method is evolved as an alternative to conventional heating. Interestingly, the reaction was completed in just 30 seconds affording the product in excellent yield (95%) with high purity.

Alternatively, an attempt was made to synthesize the pyridopyrimidine derivatives through one pot pseudo four-component reaction of 4-piperidone hydrochloride monohydrate (1), 4-methylbenzaldehyde (2) and thiourea in a molar ratio 1:2:1, respectively in presence of catalytic amount of solid sodium ethoxide (Method C). The reaction mixture in a semi-micro boiling tube was heated on a water bath with constant grinding. The reaction took quite a longer time (10 min) than the earlier methods (Method A and B) for completion, resulting a yellow viscous liquid in 61% yield. ¹H NMR analysis of this liquid showed the presence of pyridopyrimidine along with some non-characterizable impurities. In order to reduce the impurities and to lessen the reaction time, the same pseudo four-component reaction was conducted under microwave irradiation condition (method D). As expected the reaction was completed in 3–4 min affording the product along with some impurities as method C. The above results disclose that a maximum yield of pyridopyrimidine derivative was obtained with high purity when the reaction was performed under microwave irradiation method.

Structural elucidation of the pyrido-pyrimidine-2-ones (6)/pyrimidine-2-thiones (7) was accomplished by FT-IR, 1D and 2D

Figure 1. Selected HMBCs and ¹H and ¹³C chemical shifts of 7c.

6/7

Scheme 2. Mechanism for the formation of novel pyridopyrimidines 6/7.

NMR spectroscopy techniques and elemental analysis. The IR spectrum of **7c** revealed the presence of NH and C=S around 3400 and 1650 cm^{-1} , respectively. In the ^1H NMR spectrum of **7c**, the singlet at 5.47 ppm was readily assigned to H-4, which shows H,H-COSY correlations with the doublets at 3.04 and 3.28 ppm ($J = 17.90$ Hz) enabling their assignment to H-5a and H-5b. The other doublets at 3.51 and 3.66 ppm ($J = 15.09$ Hz) can be assigned to H-7a and H-7b. The one hydrogen singlet at 6.60 ppm is due to H-9 and two singlets at 7.65 and 8.08 ppm is due to two NH hydrogens while the aromatic hydrogens appeared as multiplets in the region 7.07–7.45 ppm. The assignment of signals of carbon bearing hydrogens has been done from the chemical shifts of hydrogens and C,H-COSY correlations. These assignments are also supported by the HMCs (Fig. 1) of **7c**. The ^1H and ^{13}C chemical shifts of **7c** are depicted in Figure 1. The probable mechanism for the formation of pyridopyrimidine derivatives (**6**)/(**7**) via Michael addition-condensation-tautomerization domino sequence is shown in Scheme 2.

2.2. In vitro cholinesterase enzymes inhibitory activity

The cholinesterase enzymes inhibitory activities of the synthesized compounds were summarized in Table 1. Among the twenty four newly synthesized compounds, pyridopyrimidine-2-thiones **7e** with *ortho*-methoxy and **7l** with 1-naphthyl groups on the aryl ring displayed 2.5- and 1.5-fold higher inhibitory potential against AChE in contrast to galanthamine with $\text{IC}_{50} = 0.8$ and 1.37 μM , respectively. In addition, compound **7i**, possessing *para*-chloro substituent on the aryl ring, also showed comparable AChE inhibitory potency to standard ($\text{IC}_{50} = 2.25$ μM).

Higher potency of **7e** and **7l** in contrast to standard presumably is related to high aromatic content of active site gorge in AChE enzyme. Containing electron rich aromatic cores, viz. Compound **7e** ($R = \textit{ortho}$ -methoxy) or possessing more aromatic core units as for **7l** ($R = 1\text{-naphthyl}$) facilitate insertion/accommodation of compound in the active site gorge of AChE by interactions with aromatic side chains residues that line the gorge wall.

Comparing AChE inhibitory activities of **6a–l**, comprising C=O and **7a–l** comprising C=S moieties disclosed that all derivatives of **7**, displayed better inhibitory activities than **6** except for **7c**, **7d** and **7f** which showed 1.3-, 2.2- and 1.2-fold lower activities contrasting to **6c**, **6d** and **6f**. It is worth to note that, compounds **7e**, **7i** and **7l**, significantly represented 50, 16 and 10 times more AChE inhibitory activity than their analogous **6e**, **6i** and **6l**, respectively. Remaining compounds in series **7**, also displayed 1.01–1.33 times higher inhibitory potential comparing to their resembling derivatives in series **6** as depicted in Figure 2. Lower AChE inhibitory activities observed in pyrimidinones (**6**) comparing to pyrimidinethiones (**7**) are probably attributable to hydrogen bonding interactions of electronegative oxygen atom with amino acid residues located at the entrance of AChE active site gorge which prevents the proper insertion and accommodation of inhibitors inside the gorge which is essential to expose the enzyme inhibitory activity. In series **7**, owing to displacement of oxygen atom with

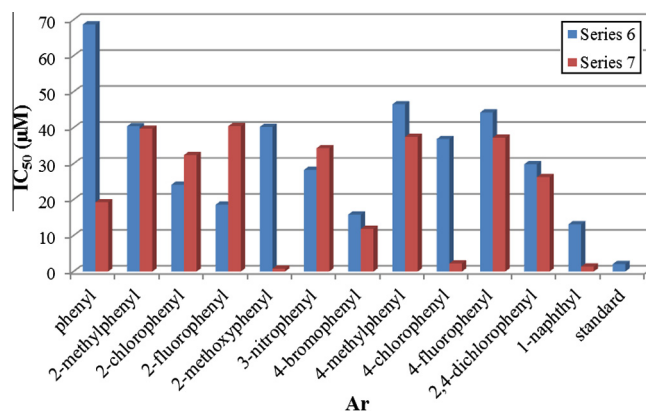


Figure 2. AChE inhibitory activity comparison diagram (IC_{50} vs substitution on aromatic ring) for **6a–l** and **7a–l**.

Table 1
Physical data, AChE and BChE activities of **6(a–l)** and **7(a–l)**

Entry	Compound	Ar	Yield (%)		AChE inhibition (IC_{50})		BChE inhibition (IC_{50})		Selectivity	
			Conv.	MWl	($\mu\text{g}/\text{ml}$)	(μM)	($\mu\text{g}/\text{ml}$)	(μM)	AChE ^a	BChE ^b
1	6a	C_6H_5	78	94	21.79 ± 0.22	68.73	0.91 ± 0.11	2.86	0.04	24.01
2	6b	2- $\text{CH}_3\text{C}_6\text{H}_4$	75	91	13.94 ± 0.14	40.42	1.80 ± 0.17	5.22	0.13	7.74
3	6c	2- ClC_6H_4	72	90	9.28 ± 0.16	24.14	0.97 ± 0.21	2.51	0.10	9.57
4	6d	2- FC_6H_4	69	89	6.56 ± 0.17	18.59	1.17 ± 0.12	3.31	0.18	5.61
5	6e	2-(OCH_3) C_6H_4	72	93	15.17 ± 0.11	40.23	4.04 ± 0.11	10.70	0.27	3.75
6	6f	3-(NO_2) C_6H_4	75	91	11.51 ± 0.12	28.27	4.21 ± 0.24	10.34	0.37	2.73
7	6g	4- BrC_6H_4	71	88	7.49 ± 0.15	15.86	2.94 ± 0.17	6.22	0.39	2.54
8	6h	4- $\text{CH}_3\text{C}_6\text{H}_4$	69	90	16.05 ± 0.15	46.52	2.45 ± 0.14	7.09	0.15	6.56
9	6i	4- ClC_6H_4	72	92	14.24 ± 0.21	36.84	6.46 ± 0.19	16.73	0.45	2.20
10	6j	4- FC_6H_4	77	94	15.61 ± 0.20	44.23	6.67 ± 0.21	18.90	0.43	2.34
11	6k	2,4- $\text{Cl}_2\text{C}_6\text{H}_3$	69	91	13.59 ± 0.22	29.86	10.77 ± 0.18	23.51	0.79	1.26
12	6l	Naphthyl	74	92	5.49 ± 0.21	13.16	2.25 ± 0.11	5.39	0.41	2.44
13	7a	C_6H_5	73	94	6.42 ± 0.14	19.27	1.26 ± 0.14	3.78	0.20	5.09
14	7b	2- $\text{CH}_3\text{C}_6\text{H}_4$	72	85	14.36 ± 0.21	39.72	1.11 ± 0.08	3.07	0.08	12.94
15	7c	2- ClC_6H_4	72	95	13.02 ± 0.17	32.39	1.17 ± 0.09	2.91	0.09	11.13
16	7d	2- FC_6H_4	72	89	14.91 ± 0.23	40.43	2.40 ± 0.10	6.50	0.16	6.21
17	7e	2-(OCH_3) C_6H_4	79	94	0.32 ± 0.05	0.80	0.46 ± 0.05	1.18	1.47	0.67
18	7f	3-(NO_2) C_6H_4	69	88	14.52 ± 0.24	34.31	3.42 ± 0.21	8.09	0.24	4.25
19	7g	4- BrC_6H_4	75	93	5.80 ± 0.18	11.88	0.81 ± 0.06	1.65	0.14	7.20
20	7h	4- $\text{CH}_3\text{C}_6\text{H}_4$	74	95	13.51 ± 0.21	37.47	2.27 ± 0.15	6.27	0.17	5.95
21	7i	4- $\text{Cl}_2\text{C}_6\text{H}_3$	72	92	1.14 ± 0.19	2.25	2.52 ± 0.10	6.26	2.78	0.35
22	7j	4- FC_6H_4	76	90	13.76 ± 0.25	37.22	10.64 ± 0.16	28.82	0.77	1.29
23	7k	2,4- $\text{Cl}_2\text{C}_6\text{H}_3$	68	91	12.27 ± 0.16	26.25	18.38 ± 0.22	49.8	1.50	0.67
24	7l	Naphthyl	67	92	0.59 ± 0.024	1.37	2.42 ± 0.17	5.58	4.07	0.25
25	Galanthamine	—	—	—	0.60 ± 0.012	2.09	5.55 ± 0.01	19.34	3.47	0.28

^a Selectivity for AChE is defined as $\text{IC}_{50}(\text{BChE})/\text{IC}_{50}(\text{AChE})$.

^b Selectivity for BChE is defined as $\text{IC}_{50}(\text{AChE})/\text{IC}_{50}(\text{BChE})$.

more polarizable sulfur atom, these unfavorable hydrogen bonding interactions are avoided and inhibitors are relatively better engrafted into the active site gorge of the enzyme resulting in higher inhibitory potencies.

As for BChE, interestingly, all the synthesized pyridopyrimidines represented selectivity toward BChE and also displayed better BChE inhibitory potential in comparison to standard drug except for **6k**, **7j** and **7k**. Analyzing IC₅₀ data represented in Table 1 disclosed that un-substituted and *ortho*-substituted derivatives in these two series demonstrated better BChE inhibitory activities in contrast to their *meta* *para* and di-substituted analogous. Additionally, compound **6a**, showed remarkable selectivity for BChE with 24 times more tendency toward this enzyme compared to AChE.

The replacement of C=O in series **6** with C=S moiety in series **7**, resulted in relatively better BChE inhibitory activity with ten compounds displaying IC₅₀ lower than 10 μM in **7** contrasting to seven compounds in **6**. Compound **6a**, **6c** and **6d**, relatively displayed better inhibitory activity compared to their analogous **7a**, **7c** and **7d**. On the other hand, *meta*- and *para*-phenyl substituted **7e–i**, showed better inhibitory activity in contrast to their analogous in series **6**. Compounds **7e** and **7g** also displayed 9 and 4 times better activities than **6e** and **6g**, respectively. Compound **6j** with *para*-fluoro phenyl and **6k** with *ortho*-, *para*-dichloro phenyl rings, relatively displayed higher potency compared to **7j** and **7k** (Fig. 3).

As mentioned earlier, unlike AChE, BChE active site wall is lined by hydrophobic residues such as leucine and valine. These changes provide more room for insertion/accommodation of substrates and inhibitors inside the BChE active site. Based on this principle, replacement of oxygen with sulfur atom in C=X moiety, does not ensue remarkable difference in inhibitory activities among similar derivatives in contrary to AChE enzyme. In both assays the maximum difference in activities among two series were observed for

ortho-methoxy phenyl derivatives, **7e** and **6e**, with IC₅₀ = 0.8 versus 40.23 μM, for AChE and IC₅₀ = 1.18 versus 10.70 μM, for BChE, respectively.

In conclusion, newly synthesized pyridopyrimidines **6** and **7** owing to their planar spatial configuration which is necessary for proper insertion into the enzymes active site and high aromatic content to facilitate accommodation of inhibitor inside the gorge through hydrophobic interaction with aromatic residues lining the active site, represented their inhibitory activity and therefore are good candidates to be used as cholinesterase inhibitor agents. Among 24 synthesized compounds, **7e** and **7i** displayed 2.5 and 1.5 times more AChE inhibitory potential compared to standard drug. It can also be noted that most of the pyridopyrimidines tested in our study were found to be 2–16 times more active and selective toward BChE in contrast to galanthamine which among them compounds **7e** and **7g** showed 16 and 12 time more activity than standard. Selective BChE may be useful in ameliorating a cholinergic deficit in AD due to increased BChE activity and its involvement in formation and maturation of β-amyloid plaques.^{9,23}

2.3. Docking simulation

In order to gain functional and structural insight into the mechanism of most active compounds, molecular docking simulation was performed by the aid of Maestro™ docking software. Active sites in TcAChE and human BChE due to different roles can be classified into five regions as mentioned in the introduction part. Amino acid residue compositions of these five sites for both enzymes are summarized in Table 2.

Molecular docking simulations were performed on TcAChE receptor for compound **7e** and **7i** which displayed superior AChE inhibitory activity in comparison to galanthamine and on hBChE receptor for compound **7e** which possessed highest BChE inhibitory activity among the newly synthesized pyridopyrimidines. This simulation may assist to reveal binding orientation and interaction of these molecules with amino acid residues composing active site gorge in these two enzymes. The interaction sites, residue involved and bonding types as well as the ligand interacting moiety are summarized in Table 3.

Molecular modeling analysis for **7e** indicated that hydrogen bonding, hydrophobic and mild polar interactions are three major interactions incorporating the attachment of this ligand to TcAChE receptor. In brief, **7e** at peripheral anionic site, represented hydrophobic interaction with Trp279, Tyr70, Tyr121 and Tyr334, at acyl binding pocket displayed hydrophobic interaction with Phe288 and Phe290 and at oxyanion hole it bound to Gly118 and Gly119 by mild polar interactions. Two π–π stacking and H-bonding interaction (2.334 Å) with Phe330 together with π–π stacking interaction with Trp84 at choline binding site, anchored this compound to the bottom of TcAChE active site gorge. In addition to interaction with residues composing peripheral anionic site, oxyanion hole, acyl binding pocket and choline binding site, this compound also displayed mild polar interactions with Glu199, Ser200 and His440 amino acid residues composing catalytic triad. Interaction of **7e** with all 5 major sites of active site gorge may be a good explanation for its remarkable AChE inhibitory activity against this enzyme

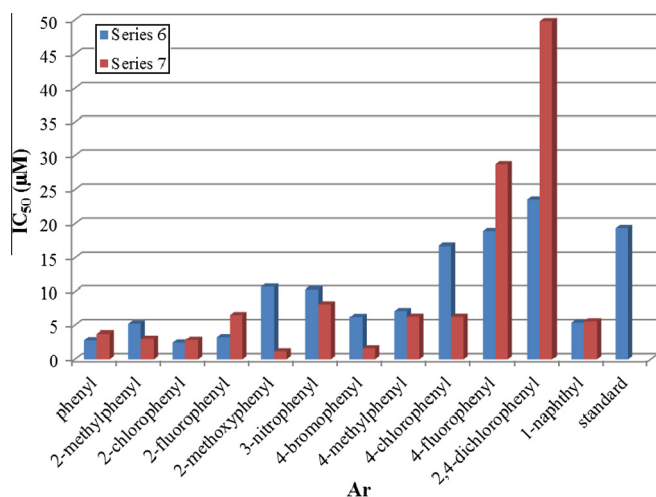


Figure 3. BChE inhibitory activity comparison diagram (IC₅₀ vs substitution on aromatic ring) for **6a–l** and **7a–l**.

Table 2

Residue composition of active sites in TcAChE and hBChE

Entry	Site name	Residue composition in TcAChE ^{28,29}	Residue composition in human BChE ¹⁴
1	Catalytic triad	Ser 200, His 440 & Glu 327	His438, Ser198 & Glu325
2	Choline binding site (α-anionic site)	Trp 84 & Phe 330	Trp82 & Phe329
3	Acyl-binding pocket	Phe 288 & Phe 290	Trp230, Leu286 & Val288
4	Oxyanion hole	Gly118, Gly119 & Ala201	Gly116, Gly117 & Ala199
5	Peripheral anionic site (β-anionic site)	Tyr 70, Asp 72, Tyr 121, Trp 279 & Tyr 334	Trp 231, Leu 286 & Phe 398

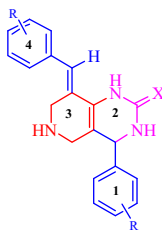
Table 3
Binding interaction data for **7e** and **7i** docked into active site gorge of AChE/**7e** docked into BChE receptors

Entry	Ligand	Enzyme	Binding energy (kcal)	Interacting site	Residue	Bond type	Residue interacting moiety	Ligand interacting moiety
1	7e	TcAChE	−10.1	PAS*	Trp 279	Hydrophobic	Indole	Ring 4
					Tyr 70	Hydrophobic	Aryl ring	Methoxy ring 4
					Tyr 334	Hydrophobic	Aryl ring	Methoxy ring 4
					Tyr 121	Hydrophobic	Methoxy	Arylidene, methoxy ring 1
					Gly 117 & 118	Mild polar	Nitrogen	Ring 1 & 2
				OH**	Phe 290	Hydrophobic	Aryl ring	Ring 4, Methoxy ring 1
					Choline binding site	Phe 330	H-bonding, π - π stacking	C=O Aryl ring
				CT***	Trp 84	π - π stacking	Indole	Ring 1
					His 440	Mild polar	Nitrogen	Ring 1
2	7i	TcAChE	−8.3	PAS	Tyr 70	Hydrophobic	Aryl ring	Ring 4
					Tyr 121	Hydrophobic	Aryl ring	Naphthyl
					Tyr 334	Hydrophobic	Aryl ring	Ring 4
					Gly 117 & 118	Mild polar	Nitrogen	Ring 1 & naphthyl
					Ala 201	Mild polar	Nitrogen	Naphthyl
				OH	Phe 290	Hydrophobic	Aryl ring	Naphthyl
					Choline binding site	Phe 330	H-bonding C=O	Nitrogen ring 3
				CT	Trp 84	π - π stacking	Indole	Ring 1
					His 440	Mild polar	Nitrogen	Ring 1
					Ser 200	Mild polar	Methoxy	Naphthyl
3	7e	hBChE	−8.7	PAS	Trp 231	Hydrophobic	Indole	Ring 4
					Phe 398	Hydrophobic	Aryl ring	Methoxy
					Val 288	Hydrophobic	Methyl	Ring 4
					Leu 286	Hydrophobic	CH ₂ & CH ₃	Ring 4
					Gly 116 & 117	Mild polar	Nitrogen	Ring 2 & 3
				OH	Ala 199	Mild polar	Nitrogen	Methoxy
					Choline binding site	Phe 329	Hydrophobic	Aryl ring
				Trp 82	Hydrophobic	Indole	Ring 1 & Methoxy	

* Peripheral anionic site.

** Oxyanion hole.

*** Catalytic triad.



in contrast to standard drug. AChE structure complexed with available Alzheimer's drugs such as huperzine A, galanthamine and tacrine also shows similar interactions of occupying of the peripheral anionic site, stacking against Trp 84 and interacting with residues at catalytic triad (Fig. 4).²⁴

Docking profile of compound **7i** closely resembles to **7e**, in which at peripheral anionic site it bound to Tyr70, Tyr121, Tyr334 and Trp279 residues through hydrophobic interactions and strongly anchored to choline binding site through hydrophobic and hydrogen bonding (2.30 Å) interactions with Phe330 beside π - π stacking interaction with Trp84. This compound also showed mild polar interaction with Gly188, Gly119 and Ala201 at oxyanion hole and Ser200 and His440 at catalytic triad. As mentioned earlier these key interactions are also observable in AChE crystal structure complexed with available Alzheimer's drugs (Fig. 5).

Docking of compound **7e** on hBChE receptor showed hydrophobic interaction with Trp231, Phe398, Val288 and Leu286 at peripheral anionic site beside Phe329 and Trp82 at choline binding site together with mild polar interactions with Gly 116, Gly 117 and Ala 199 at oxyanion hole. This compound also attached to side chain residues such as Tyr 332 and Trp 430 at the bottom of the gorge (Fig. 6).

In conclusion, information gathered from docking simulation analysis for **7e** and **7i** were in accordance with the IC₅₀ values obtained from the cholinesterase inhibition assay. In general, better accommodation of inhibitor inside the active site gorge due to more appropriate interactions with its amino acid residues, ensue better inhibitory activities and lower IC₅₀ values during In vitro assay.

3. Conclusion

In conclusion a series of pyridopyrimidine derivatives were synthesized employing a facile microwave irradiation protocol and were assayed for their AChE and BChE activities. Compound **7e** displayed the highest inhibition for both AChE and BChE enzymes with IC₅₀ of 0.8 and 1.18 μ M, respectively. Compound **7i** also displayed higher inhibitory potential for AChE in comparison to galanthamine with IC₅₀ = 1.37 μ M. 21 out of 24 compounds in this series, represented higher inhibitory activities toward BChE in contrast to galanthamine ranging from 1.18 to 18.90 μ M. Molecular docking of **7e** and **7i** to TcAChE and hBChE receptors completely coincided with the activities observed. The presence of NH, C=S/O and C=C functionalities in these pyridopyrimidine derivatives makes it a valuable synthon for the construction of more complex heterocycles of biological importance.

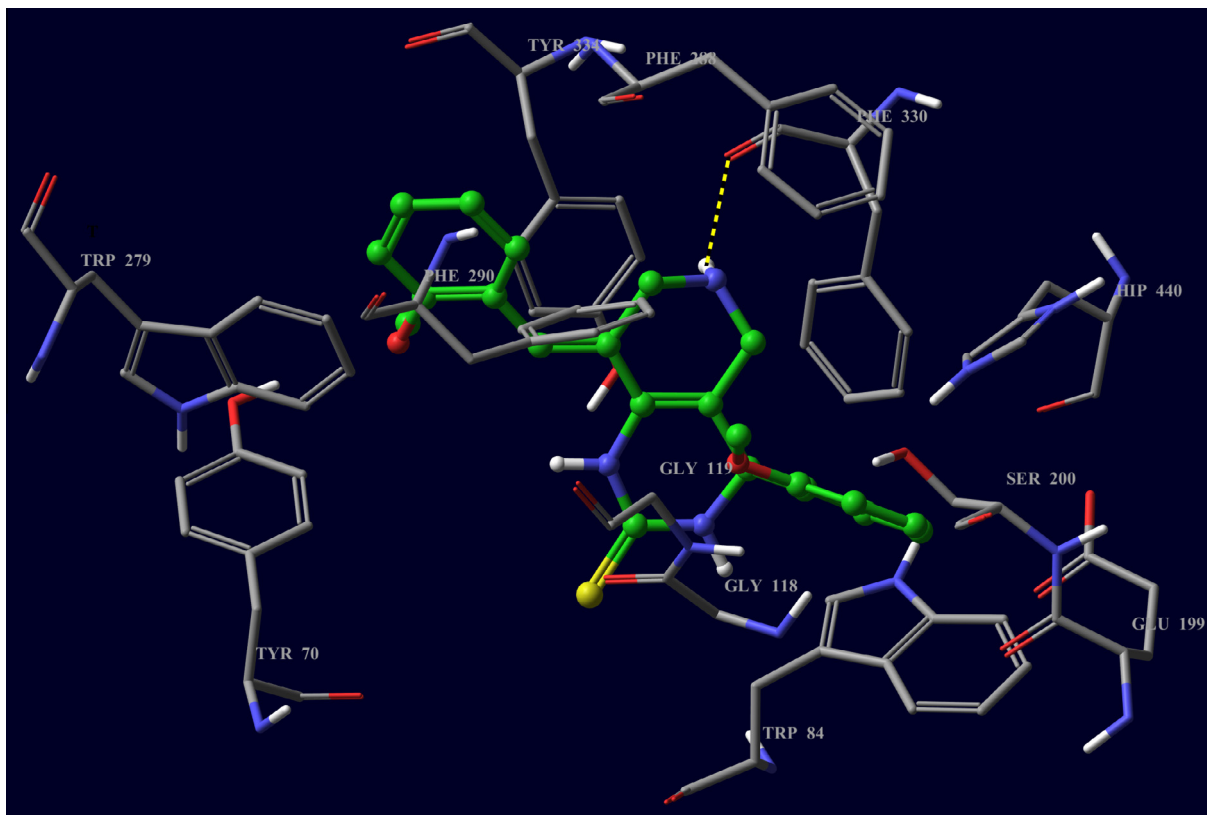


Figure 4. Binding interaction of **7e** with active site residues of TcAChE receptor.

4. Experimental

4.1. General methods

The chemicals used were obtained from Merck (Germany) and Sigma Aldrich (USA). Melting points were determined by open tube capillary method and are uncorrected. A CEM microwave synthesizer (Model: Discover-S 908860) operating at 180/240 V and 50/60 Hz with consumption of 1100 W with microwave power maximum level of 300 W and microwave frequency of 2455 MHz was employed for the irradiation done in this work. Purity of the compounds was checked on thin layer chromatography (TLC) plates (silica gel G) using the petroleum ether/ethyl acetate solvent system and the spots were examined under UV light. ^1H and ^{13}C NMR were performed on Bruker Avance 500 (^1H : 500 MHz, ^{13}C : 125 MHz) spectrometer in CDCl_3 , using TMS as internal standard.

4.2. General procedure for synthesis of **6** and **7**

Conventional method: Catalytic amount of sodium ethoxide was added to an equimolar dry mixture of unsaturated ketones (**3**) and urea/thiourea (**4** and **5**), the mixture was ground uniformly in a semi-micro boiling tube on the water bath for about 4–5 min during which period a transparent viscous liquid formed showing completion of reaction and double examined by TLC. Water was added to the mixture, precipitated solid was filtered and dried in vacuo to afford compounds **6a–I** and **7a–I** in moderate to good yields (Table 1).

Microwave irradiation method: Catalytic amount of sodium ethoxide was added to an equimolar dry mixture of unsaturated ketones (**3**) and urea/thiourea (**4** and **5**), the mixture was ground well in a semi-micro boiling tube and irradiated for 0.5 min in a CEM microwave synthesizer during which period a transparent viscous liquid formed showing completion of reaction and double

examined by TLC. Water was added to the mixture, precipitated solid was filtered and dried in vacuo to afford compounds **6a–I** and **7a–I** in excellent yields (Table 1).

4.2.1. (*E*)-8-(2-Benzylidene-4-phenyl-3,4,5,6,7,8-hexahydropyrido[4,3-*d*]pyrimidin-2(1*H*)-one (**6a**)

Yellow solid; mp 130–132 °C; Anal. Calcd for $\text{C}_{20}\text{H}_{19}\text{N}_3\text{O}$: C, 75.69; H, 6.03; N, 13.24. Found: 75.24; H, 5.62; N, 13.02. ^1H NMR (500 MHz, CDCl_3): δ_{H} 2.96 (d, 1H, $J = 17.25$ Hz, H-5a), 3.13 (d, 1H, $J = 17.25$ Hz, H-5b), 3.60 (d, 1H, $J = 15.10$ Hz, H-7a), 3.76 (d, 1H, $J = 15.10$ Hz, H-7b), 4.80 (s, 1H, H-4), 6.34 (s, 1H, NH), 6.71 (s, 1H, H-9), 7.13–7.35 (m, 10H, H-aromatic, NH), 7.95 (s, 1H, NH); ^{13}C NMR (125 MHz, CDCl_3): δ_{C} 45.29, 45.38, 50.09, 110.77, 121.87, 126.99, 128.27, 128.99, 129.35, 136.24, 142.34, 154.28.

4.2.2. (*E*)-8-(2-Methylbenzylidene)-4-*p*-tolyl-3,5,6,7,8-hexahydropyrido[4,3-*d*]pyrimidin-2(1*H*)-one (**6b**)

Yellow solid; mp 154–156 °C; Anal. Calcd for $\text{C}_{22}\text{H}_{23}\text{N}_3\text{O}$: C, 76.49; H, 6.71; N, 12.16. Found: 76.94; H, 6.12; N, 12.21. ^1H NMR (500 MHz, CDCl_3): δ_{H} 2.31 (s, 3H, CH_3), 2.45 (s, 3H, CH_3), 2.98 (d, 1H, $J = 17.14$ Hz, H-5a), 3.18 (d, 1H, $J = 17.14$ Hz, H-5b), 3.57 (d, 1H, $J = 15.04$ Hz, H-7a), 3.69 (d, 1H, $J = 15.04$ Hz, H-7b), 5.26 (s, 1H, H-4), 5.63 (s, 1H, NH), 6.69 (s, 1H, H-9), 7.03–7.35 (m, 9H, aromatic, NH); ^{13}C NMR (125 MHz, CDCl_3): δ_{C} 19.51, 20.50, 45.75, 45.92, 56.65, 110.55, 120.87, 125.80, 127.31, 127.93, 128.40, 128.68, 128.84, 129.77, 130.45, 131.56, 135.51, 135.87, 137.36, 139.75, 154.13.

4.2.3. (*E*)-8-(2-Chlorobenzylidene)-4-(2-chlorophenyl)-3,4,5,6,7,8-hexahydropyrido[4,3-*d*]pyrimidin-2(1*H*)-one (**6c**)

Yellow solid; mp 155–157 °C; Anal. Calcd for $\text{C}_{20}\text{H}_{17}\text{Cl}_2\text{N}_3\text{O}$: C, 62.19; H, 4.44; N, 10.88. Found: 62.37; H, 4.12; N, 10.77. ^1H NMR (500 MHz, CDCl_3): δ_{H} 3.11 (d, 1H, $J = 17.46$ Hz, H-5a), 3.36 (d, 1H, $J = 17.46$ Hz, H-5b), 3.60 (d, 1H, $J = 14.94$ Hz, H-7a), 3.72

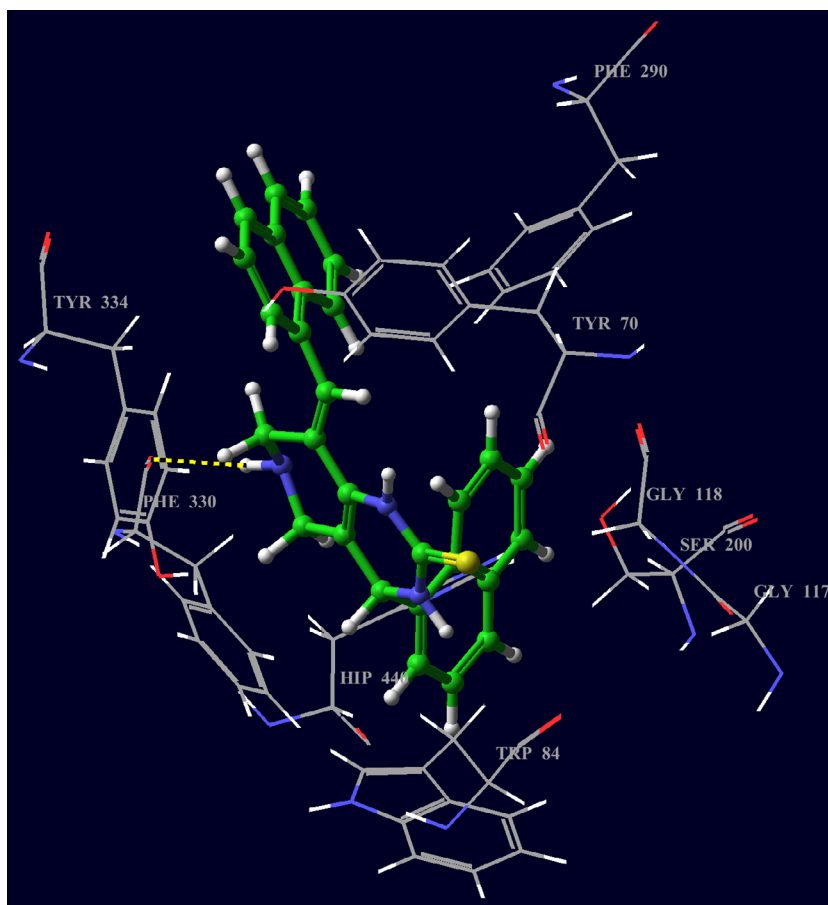


Figure 5. Binding Interaction of 71 with active site residues of TcAChE receptor.

(d, 1H, $J = 14.94$ Hz, H-7b), 5.50 (s, 1H, H-4), 5.73 (s, 1H, NH), 6.73 (s, 1H, H-9), 7.12–7.47 (m, 9H, aromatic, NH); ^{13}C NMR (125 MHz, CDCl_3): δ_{C} 45.68, 45.82, 55.20, 110.86, 119.33, 126.76, 128.37, 128.59, 129.18, 129.59, 129.77, 130.01, 130.20, 131.25, 133.04, 134.44, 139.12, 154.07.

4.2.4. (*E*)-8-(2-Fluorobenzylidene)-4-(2-fluorophenyl)-3,4,5,6,7,8-hexahydropyrido[4,3-*d*]pyrimidin-2(1*H*)-one (6d)

Yellow solid; mp 146–149 °C; Anal. Calcd for $\text{C}_{20}\text{H}_{17}\text{F}_2\text{N}_3\text{O}$ C, 67.98; H, 4.85; N, 11.89. Found: C, 67.74; H, 4.75; N, 12.10. ^1H NMR (500 MHz, CDCl_3): δ_{H} 3.13 (d, 1H, $J = 17.46$ Hz, H-5a), 3.32 (d, 1H, $J = 17.46$ Hz, H-5b), 3.57 (d, 1H, $J = 15.09$ Hz, H-7a), 3.71 (d, 1H, $J = 15.09$ Hz, H-7b), 5.30 (s, 1H, H-4), 6.00 (s, 1H, NH), 6.65 (s, 1H, H-9), 6.97–7.40 (m, 8H, H-aromatic), 7.73 (s, 1H, NH); ^{13}C NMR (125 MHz, CDCl_3): δ_{C} 45.57, 45.97, 110.54, 114.91, 115.82, 115.90, 116.12, 116.18, 124.14, 124.19, 124.31, 125.38, 125.43, 128.28, 129.07, 129.11, 129.28, 129.57, 129.67, 130.26, 130.37, 131.25, 131.28, 154.54, 158.65, 158.82, 161.92, 162.11.

4.2.5. (*E*)-8-(2-Methoxybenzylidene)-4-(2-methoxyphenyl)-3,4,5,6,7,8-hexahydropyrido[4,3-*d*]pyrimidin-2(1*H*)-one (6e)

Yellow solid; mp 182–184 °C; Anal. Calcd for $\text{C}_{22}\text{H}_{23}\text{N}_3\text{O}_3$ C, 70.01; H, 6.14; N, 11.13. Found: C, 70.42; H, 6.01; N, 11.64. ^1H NMR (500 MHz, CDCl_3): δ_{H} 3.23 (d, 1H, $J = 17.58$ Hz, H-5a), 3.34 (d, 1H, $J = 17.58$ Hz, H-5b), 3.70 (d, 1H, $J = 15.06$ Hz, H-7a), 3.82 (d, 1H, $J = 15.06$ Hz, H-7b), 3.83 (s, 3H, OCH_3), 3.84 (s, 3H, OCH_3), 5.35 (s, 1H, H-4), 5.61 (s, 1H, NH), 6.65 (s, 1H, H-9), 6.87–7.30 (m, 9H, aromatic, NH); ^{13}C NMR (125 MHz, CDCl_3): δ_{C} 46.05, 52.19, 55.74, 55.77, 110.30, 110.85, 110.99, 116.84, 120.48, 121.48, 125.17, 127.99, 128.45, 128.86, 129.33, 129.66, 129.71, 130.79, 154.60, 157.00, 157.63.

4.2.6. (*E*)-8-(3-Nitrobenzylidene)-4-(3-nitrophenyl)-3,4,5,6,7,8-hexahydropyrido[4,3-*d*]pyrimidin-2(1*H*)-one (6f)

Yellow solid; mp 176–178 °C; Anal. Calcd for $\text{C}_{20}\text{H}_{17}\text{N}_5\text{O}_5$ C, 58.97; H, 4.21; N, 17.19. Found: C, 58.17; H, 4.29; N, 17.11. ^1H NMR (500 MHz, CDCl_3): δ_{H} 2.73 (d, 1H, $J = 18.06$ Hz, H-5a), 3.01 (d, 1H, $J = 18.06$ Hz, H-5b), 3.34 (d, 1H, $J = 15.24$ Hz, H-7a), 3.54 (d, 1H, $J = 15.24$ Hz, H-7b), 4.99 (s, 1H, H-4), 5.48 (s, 1H, NH), 6.02 (s, 1H, H-9), 7.10–8.08 (m, 8H, aromatic), 8.31 (s, 1H, NH); ^{13}C NMR (125 MHz, CDCl_3): δ_{C} 45.73, 45.97, 111.03, 119.99, 122.96, 125.36, 125.45, 125.94, 126.24, 126.33, 126.49, 127.09, 127.38, 128.22, 128.74, 129.46, 129.70, 131.10, 132.29, 133.62, 133.87, 134.49, 154.47.

4.2.7. (*E*)-8-(4-Bromobenzylidene)-4-(4-bromophenyl)-3,4,5,6,7,8-hexahydropyrido[4,3-*d*]pyrimidine-2(1*H*)-one (6g)

Yellow solid; mp 174–176 °C; Anal. Calcd for $\text{C}_{20}\text{H}_{17}\text{Br}_2\text{N}_3\text{O}$ C, 48.90; H, 3.49; N, 8.55. Found: C, 49.25; H, 4.05; N, 8.21. ^1H NMR (500 MHz, CDCl_3): δ_{H} 2.91 (d, 1H, $J = 11.05$ Hz, H-5a), 3.09 (d, 1H, $J = 11.05$ Hz, H-5b), 3.54 (d, 1H, $J = 9.15$ Hz, H-7a), 3.64 (d, 1H, $J = 9.15$ Hz, H-7b), 4.87 (s, 1H, H-4), 6.39 (s, 1H, NH), 6.61 (s, 1H, H-9), 7.05–7.31 (m, 8H, H-aromatic), 8.01 (s, 1H, NH); ^{13}C NMR (125 MHz, CDCl_3): δ_{C} 45.22, 45.29, 58.46, 110.69, 120.72, 127.25, 128.31, 128.39, 128.52, 129.17, 130.44, 133.05, 134.21, 134.52, 140.54, 154.07.

4.2.8. (*E*)-8-(4-Methylbenzylidene)-4-*p*-tolyl-3,4,5,6,7,8-hexahydropyrido[4,3-*d*]pyrimidin-2(1*H*)-one (6h)

Yellow solid; mp 170–173 °C; Anal. Calcd for $\text{C}_{22}\text{H}_{23}\text{N}_3\text{O}$ C, 76.49; H, 6.71; N, 12.16. Found: C, 76.91; H, 6.77; N, 11.85. ^1H NMR (500 MHz, CDCl_3): δ_{H} 2.35 (br.s, 6H, CH_3), 3.04 (d, 1H, $J = 17.28$ Hz, H-5a), 3.21 (d, 1H, $J = 17.28$ Hz, H-5b), 3.69 (d, 1H,

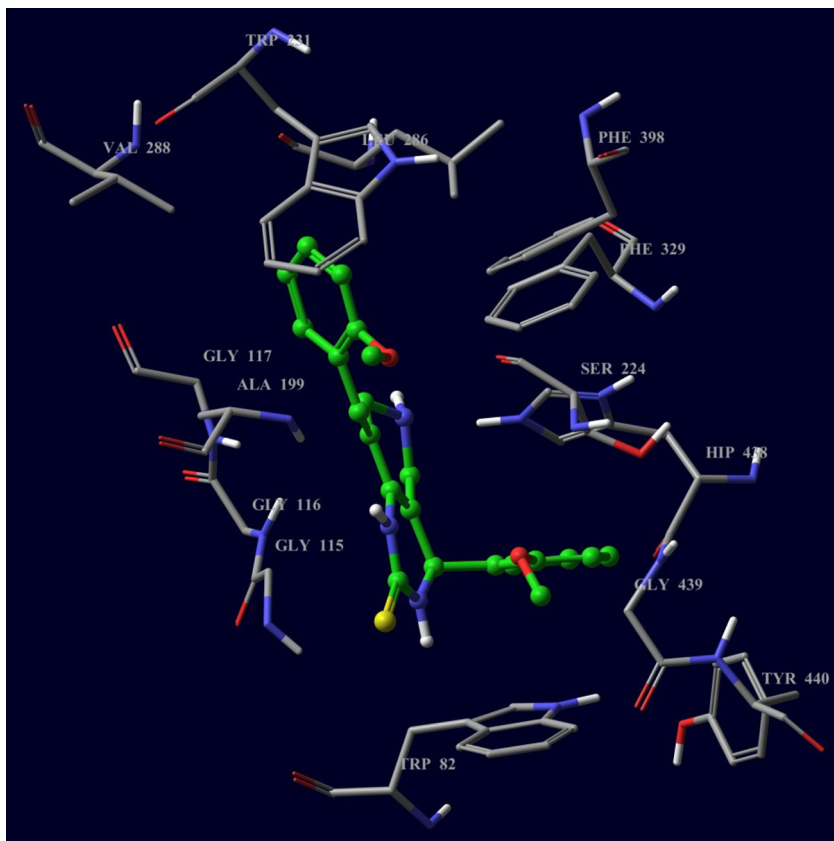


Figure 6. Binding interaction of **7e** with active site of hBChE receptor.

$J = 15.09$ Hz, H-7a), 3.85 (d, 1H, $J = 15.09$ Hz, H-7b), 4.88 (s, 1H, H-4), 5.80 (s, 1H, NH), 6.60 (s, 1H, H-9), 7.07–7.36 (m, 8H, H-aromatic); ^{13}C NMR (125 MHz, CDCl_3): δ_{C} 21.53, 21.60, 45.73, 45.86, 59.38, 111.10, 121.70, 127.29, 127.98, 129.41, 129.66, 130.07, 133.60, 137.51, 138.59, 139.70, 154.20.

4.2.9. (E)-8-(4-Chlorobenzylidene)-4-(4-chlorophenyl)-3,4,5,6,7,8-hexahydropyrido[4,3-d]pyrimidin-2(1H)-one (6i)

Yellow solid; mp 170–172 °C; Anal. Calcd for $\text{C}_{20}\text{H}_{17}\text{Cl}_2\text{N}_3\text{O}$ C, 62.19; H, 4.44; N, 10.88. Found: C, 62.72; H, 4.25; N, 10.57. ^1H NMR (500 MHz, CDCl_3): δ_{H} 2.96 (d, 1H, $J = 10.29$ Hz, H-5a), 3.15 (d, 1H, $J = 10.29$ Hz, H-5b), 3.62 (d, 1H, $J = 8.97$ Hz, H-7a), 3.75 (d, 1H, $J = 8.97$ Hz, H-7b), 4.83 (s, 1H, H-4), 6.37 (s, 1H, NH), 6.64 (s, 1H, H-9), 7.07–7.27 (m, 8H, H-aromatic), 8.02 (s, 1H, NH); ^{13}C NMR (125 MHz, CDCl_3): δ_{C} 45.27, 45.34, 58.46, 110.76, 120.81, 127.31, 128.33, 128.45, 128.60, 129.24, 130.58, 133.08, 134.29, 134.56, 140.63, 154.10.

4.2.10. (E)-8-(4-Fluorobenzylidene)-4-(4-fluorophenyl)-3,4,5,6,7,8-hexahydropyrido[4,3-d]pyrimidin-2(1H)-one (6j)

Yellow solid; mp 156–158 °C; Anal. Calcd for $\text{C}_{20}\text{H}_{17}\text{F}_2\text{N}_3\text{O}$ C, 67.98; H, 4.85; N, 11.89. Found: C, 67.78; H, 4.81; N, 11.88. ^1H NMR (500 MHz, CDCl_3): δ_{H} 2.98 (d, 1H, $J = 10.32$ Hz, H-5a), 3.16 (d, 1H, $J = 10.32$ Hz, H-5b), 3.64 (d, 1H, $J = 9.03$ Hz, H-7a), 3.75 (d, 1H, $J = 9.03$ Hz, H-7b), 4.85 (s, 1H, H-4), 6.33 (s, 1H, NH), 6.648 (s, 1H, H-9), 6.92–7.24 (m, 8H, H-aromatic), 8.00 (s, 1H, NH); ^{13}C NMR (125 MHz, CDCl_3): δ_{C} 45.27, 45.41, 58.36, 110.61, 115.15, 115.32, 115.84, 116.01, 120.90, 127.26, 127.82, 128.65, 128.72, 130.95, 131.02, 132.22, 132.24, 138.08, 138.10, 154.15, 160.85, 161.64, 162.82, 163.61.

4.2.11. (E)-8-(2,4-Dichlorobenzylidene)-4-(2,4-dichlorophenyl)-3,4,5,6,7,8-hexahydropyrido[4,3-d]pyrimidin-2(1H)-one (6k)

Yellow solid; mp 160–162 °C; Anal. Calcd for $\text{C}_{20}\text{H}_{15}\text{Cl}_4\text{N}_3\text{O}$ C, 52.78; H, 3.32; N, 9.23. Found: C, 52.31; H, 3.82; N, 8.99. ^1H NMR (500 MHz, CDCl_3): δ_{H} 3.08 (d, 1H, $J = 18.00$ Hz, H-5a), 3.34 (d, 1H, $J = 18.00$ Hz, H-5b), 3.56 (d, 1H, $J = 14.07$ Hz, H-7a), 3.67 (d, 1H, $J = 14.07$ Hz, H-7b), 4.70 (s, 1H, H-4), 5.87 (s, 1H, NH), 6.66 (s, 1H, H-9), 7.03–7.41 (m, 6H, H-aromatic), 7.72 (s, 1H, NH); ^{13}C NMR (125 MHz, CDCl_3): δ_{C} 45.56, 45.76, 54.81, 110.78, 118.62, 127.14, 127.60, 128.63, 128.75, 129.90, 130.05, 130.48, 131.82, 133.13, 133.62, 134.38, 135.10, 135.28, 137.70, 153.99.

4.2.12. (E)-4-(Naphthalen-1-yl)-8-(naphthalen-1-ylmethylene)-3,4,5,6,7,8-hexahydropyrido[4,3-d]pyrimidin-2(1H)-one (6l)

Yellow solid; mp 175–177 °C; Anal. Calcd for $\text{C}_{28}\text{H}_{23}\text{N}_3\text{O}$ C, 80.55; H, 5.55; N, 10.06. Found: C, 80.27; H, 5.19; N, 10.21. ^1H NMR (500 MHz, CDCl_3): δ_{H} 3.14 (d, 1H, $J = 17.05$ Hz, H-5a), 3.27 (d, 1H, $J = 17.05$ Hz, H-5b), 3.82 (d, 1H, $J = 15.14$ Hz, H-7a), 3.97 (d, 1H, $J = 15.14$ Hz, H-7b), 4.92 (s, 1H, H-4), 5.85 (s, 1H, NH), 6.63 (s, 1H, H-9), 6.87–7.92 (m, 15H, H-aromatic, NH); ^{13}C NMR (125 MHz, CDCl_3): δ_{C} 45.67, 45.74, 59.41, 111.17, 121.74, 127.31, 125.6, 125.8, 126.44, 127.98, 129.48, 129.76, 130.07, 133.35, 133.69, 137.51, 138.71, 139.77, 153.12.

4.2.13. (E)-8-Benzylidene-4-phenyl-3,4,5,6,7,8-hexahydropyrido[4,3-d]pyrimidin-2(1H)-thione (7a)

Yellow solid; mp 130–132 °C; Anal. Calcd for $\text{C}_{20}\text{H}_{19}\text{N}_3\text{S}$ C, 72.04; H, 5.74; N, 12.60. Found: C, 71.68; H, 5.57; N, 12.15. ^1H NMR (500 MHz, CDCl_3): δ_{H} 3.01 (d, 1H, $J = 17.07$ Hz, H-5a), 3.21 (d, 1H, $J = 17.07$ Hz, H-5b), 3.60 (d, 1H, $J = 15.18$ Hz, H-7a), 3.82

(d, 1H, $J = 15.18$ Hz, H-7b), 4.90 (s, 1H, H-4), 6.59 (s, 1H, H-9), 7.10–7.38 (m, 11H, H-aromatic, NH), 7.94 (s, 1H, NH); ^{13}C NMR (125 MHz, CDCl_3): δ_{C} 45.40, 45.49, 59.40, 112.90, 122.32, 126.08, 127.38, 127.52, 127.99, 128.84, 129.22, 129.52, 129.67, 135.88, 141.23, 174.45.

4.2.14. (E)-8-(2-Methylbenzylidene)-4-o-tolyl-3,4,5,6,7,8-hexahydropyrido[4,3-d]pyrimidine-2(1H)-thione (7b)

Yellow solid; mp 128–130 °C; Anal. Calcd for $\text{C}_{22}\text{H}_{23}\text{N}_3\text{S}$ C, 73.09; H, 6.41; N, 11.62. Found: C, 72.88; H, 6.21; N, 11.77. ^1H NMR (500 MHz, CDCl_3): δ_{H} 2.26 (s, 3H, CH_3), 2.34 (s, 3H, CH_3), 2.85 (d, 1H, $J = 17.25$ Hz, H-5a), 3.11 (d, 1H, $J = 17.25$ Hz, H-5b), 3.36 (d, 1H, $J = 15.09$ Hz, H-7a), 3.57 (d, 1H, $J = 15.09$ Hz, H-7b), 5.18 (s, 1H, H-4), 6.59 (s, 1H, H-9), 6.59–7.28 (m, 9H, H-aromatic, NH), 7.73 (s, 1H, NH); ^{13}C NMR (125 MHz, CDCl_3): δ_{C} 19.68, 20.54, 45.19, 45.45, 56.48, 112.26, 121.32, 125.96, 126.25, 127.40, 128.26, 129.04, 129.13, 129.79, 130.54, 131.64, 134.93, 136.02, 137.15, 138.60, 174.24.

4.2.15. (E)-8-(2-Chlorobenzylidene)-4-(2-chlorophenyl)-3,4,5,6,7,8-hexahydropyrido[4,3-d]pyrimidine-2(1H)-thione (7c)

Yellow solid; mp 130–133 °C; Anal. Calcd for $\text{C}_{20}\text{H}_{17}\text{Cl}_2\text{N}_3\text{S}$ C, 59.70; H, 4.26; N, 10.44. Found: C, 59.19; H, 3.74; N, 10.21. ^1H NMR (500 MHz, CDCl_3): δ_{H} 2.12 (br.s 1H, NH), 3.04 (d, 1H, $J = 17.90$ Hz, H-5a), 3.28 (d, 1H, $J = 17.90$ Hz, H-5b), 3.51 (d, 1H, $J = 15.09$ Hz, H-7a), 3.66 (d, 1H, $J = 15.09$ Hz, H-7b), 5.47 (s, 1H, H-4), 6.60 (s, 1H, H-9), 7.07–7.45 (m, 9H, aromatic, H-arylmethylidene), 7.65 (s, 1H, NH), 8.08 (s, 1H, NH); ^{13}C NMR (125 MHz, CDCl_3): δ_{C} 45.05, 45.79, 54.78, 112.54, 119.41, 126.54, 128.13, 129.12, 129.56, 129.67, 129.95, 130.03, 130.87, 132.59, 133.73, 133.91, 137.61, 174.35.

4.2.16. (E)-8-(2-Fluorobenzylidene)-4-(2-fluorophenyl)-3,4,5,6,7,8-hexahydropyrido[4,3-d]pyrimidine-2(1H)-thione (7d)

Yellow solid; mp 128–130 °C; Anal. Calcd for $\text{C}_{20}\text{H}_{17}\text{F}_2\text{N}_3\text{S}$ C, 65.02; H, 4.64; N, 11.37. Found: C, 65.71; H, 4.39; N, 11.28. ^1H NMR (500 MHz, CDCl_3): δ_{H} 3.15 (d, 1H, $J = 17.76$ Hz, H-5a), 3.33 (d, 1H, $J = 17.76$ Hz, H-5b), 3.57 (d, 1H, $J = 15.09$ Hz, H-7a), 3.72 (d, 1H, $J = 15.09$ Hz, H-7b), 5.33 (s, 1H, H-4), 6.57 (s, 1H, H-9) 7.00–7.38 (m, 8H, aromatic), 7.42 (s, 1H, NH), 7.98 (s, 1H, NH); δ_{C} 45.32, 45.72, 52.01, 52.07, 112.26, 115.14, 115.17, 115.96, 116.10, 116.25, 116.39, 123.46, 123.65, 124.30, 124.35, 125.60, 125.65, 126.81, 127.80, 127.98, 129.24, 129.29, 130.00, 130.11, 130.84, 130.95, 131.15, 131.19, 158.55, 158.81, 161.83, 162.10, 175.22.

4.2.17. (E)-8-(2-Methoxybenzylidene)-4-(2-methoxyphenyl)-3,4,5,6,7,8-hexahydropyrido[4,3-d]pyrimidine-2(1H)-thione (7e)

Yellow solid; mp 190–192 °C; Anal. Calcd for $\text{C}_{22}\text{H}_{23}\text{N}_3\text{O}_2\text{S}$ C, 67.15; H, 5.89; N, 10.68. Found: C, 67.22; H, 5.93; N, 10.67. ^1H NMR (500 MHz, CDCl_3): δ_{H} 3.22 (d, 1H, $J = 17.85$ Hz, H-5a), 3.30 (d, 1H, $J = 17.85$ Hz, H-5b), 3.67 (d, 1H, $J = 15.99$ Hz, H-7a), 3.79 (d, 1H, $J = 15.99$ Hz, H-7b), 3.84 (s, 3H, OCH_3), 3.85 (s, 3H, OCH_3), 5.38 (s, 1H, H-4), 6.67 (s, 1H, H-9), 6.88–7.32 (m, 9H, aromatic and NH), 7.82 (s, 1H, NH); ^{13}C NMR (125 MHz, CDCl_3): δ_{C} 45.78, 45.92, 52.35, 55.74, 55.86, 110.86, 111.15, 111.73, 117.56, 120.51, 121.62, 124.67, 127.25, 127.59, 128.27, 128.35, 129.40, 129.63, 130.22, 130.59, 130.79, 156.91, 157.65, 175.03.

4.2.18. (E)-8-(3-Nitrobenzylidene)-4-(3-nitrophenyl)-3,4,5,6,7,8-hexahydropyrido[4,3-d]pyrimidine-2(1H)-thione (7f)

Yellow solid; mp 180–183 °C; Anal. Calcd for $\text{C}_{20}\text{H}_{17}\text{N}_5\text{O}_4\text{S}$ C, 56.73; H, 4.05; N, 16.54. Found: C, 56.17; H, 3.72; N, 16.02. ^1H NMR (500 MHz, CDCl_3): δ_{H} 2.83 (d, 1H, $J = 17.79$ Hz, H-5a), 3.14 (d, 1H, $J = 17.79$ Hz, H-5b), 3.39 (d, 1H, $J = 15.00$ Hz, H-7a), 3.61

(d, 1H, $J = 15.00$ Hz, H-7b), 5.59 (s, 1H, H-4), 7.12 (s, 1H, H-9), 7.15–8.06 (m, 9H, aromatic and NH), 8.21 (s, 1H, NH); ^{13}C NMR (125 MHz, CDCl_3): δ_{C} 45.49, 45.80, 112.84, 120.22, 122.58, 125.12, 125.57, 126.02, 126.53, 126.59, 126.67, 126.84, 127.51, 127.59, 128.75, 128.84, 129.00, 129.68, 130.07, 131.00, 132.13, 132.85, 133.96, 134.51, 135.60, 174.76.

4.2.19. (E)-8-(4-Bromobenzylidene)-4-(4-bromophenyl)-3,4,5,6,7,8-hexahydropyrido[4,3-d]pyrimidine-2(1H)-thione (7g)

Yellow solid; mp 139–142 °C; Anal. Calcd for $\text{C}_{20}\text{H}_{17}\text{Br}_2\text{N}_3\text{S}$ C, 50.55; H, 3.61; N, 8.84. Found: C, 50.15; H, 3.21; N, 8.49. ^1H NMR (500 MHz, CDCl_3): δ_{H} 2.93 (d, 1H, $J = 11.09$ Hz, H-5a), 3.12 (d, 1H, $J = 11.09$ Hz, H-5b), 3.57 (d, 1H, $J = 9.05$ Hz, H-7a), 3.69 (d, 1H, $J = 9.05$ Hz, H-7b), 5.39 (s, 1H, H-4), 7.08 (s, 1H, H-9), 7.07–7.49 (m, 8H, H-aromatic), 8.17 (s, 1H, NH); ^{13}C NMR (125 MHz, CDCl_3): δ_{C} 45.41, 45.82, 59.11, 111.69, 121.82, 127.94, 128.82, 129.12, 129.46, 129.89, 131.43, 133.75, 134.79, 135.21, 140.54, 175.15.

4.2.20. (E)-8-(4-Methylbenzylidene)-4-p-tolyl-3,4,5,6,7,8-hexahydropyrido[4,3-d]pyrimidine-2(1H)-thione (7h)

Yellow solid; mp 134–137 °C; Anal. Calcd for $\text{C}_{22}\text{H}_{23}\text{N}_3\text{S}$ C, 73.09; H, 6.41; N, 11.62. Found: C, 72.51; H, 6.18; N, 11.45. ^1H NMR (500 MHz, CDCl_3): δ_{H} 2.34 (s, 3H, CH_3), 2.36 (s, 3H, CH_3), 3.04 (d, 1H, $J = 17.68$ Hz, H-5a), 3.21 (d, 1H, $J = 17.68$ Hz, H-5b), 3.63 (d, 1H, $J = 14.37$ Hz, H-7a), 3.83 (d, 1H, $J = 14.37$ Hz, H-7b), 4.88 (s, 1H, H-4), 6.55 (s, 1H, H-9), 6.75–7.49 (m, 9H, aromatic and NH), 7.87 (s, 1H, NH); ^{13}C NMR (125 MHz, CDCl_3): δ_{C} 21.57, 21.64, 45.40, 45.59, 59.17, 112.70, 122.13, 125.98, 126.71, 127.35, 127.44, 129.55, 129.63, 130.17, 130.23, 133.00, 137.93, 138.34, 139.07, 174.42.

4.2.21. (E)-8-(4-Chlorobenzylidene)-4-(4-chlorophenyl)-3,4,5,6,7,8-hexahydropyrido[4,3-d]pyrimidine-2(1H)-thione (7i)

Yellow solid; mp 142–147 °C; Anal. Calcd for $\text{C}_{20}\text{H}_{17}\text{Cl}_2\text{N}_3\text{S}$ C, 59.70; H, 4.26; N, 10.44. Found: C, 59.92; H, 4.42; N, 10.31. ^1H NMR (500 MHz, CDCl_3): δ_{H} 3.00 (d, 1H, $J = 17.58$ Hz, H-5a), 3.23 (d, 1H, $J = 17.58$ Hz, H-5b), 3.58 (d, 1H, $J = 15.06$ Hz, H-7a), 3.79 (d, 1H, $J = 15.06$ Hz, H-7b), 4.89 (s, 1H, H-4), 6.58 (s, 1H, H-9), 7.05–7.34 (m, 8H, aromatic), 7.93 (s, 1H, NH), 8.07 (s, 1H, NH); ^{13}C NMR (125 MHz, CDCl_3): δ_{C} 45.39, 45.51, 58.63, 112.93, 126.22, 127.72, 128.87, 129.08, 129.80, 130.94, 133.95, 134.26, 135.12, 139.69, 174.31.

4.2.22. (E)-8-(4-Fluorobenzylidene)-4-(4-fluorophenyl)-3,4,5,6,7,8-hexahydropyrido[4,3-d]pyrimidine-2(1H)-thione (7j)

Yellow solid; mp 140–142 °C; Anal. Calcd for $\text{C}_{20}\text{H}_{17}\text{F}_2\text{N}_3\text{S}$ C, 65.02; H, 4.64; N, 11.37. Found: C, 65.29; H, 4.91; N, 11.15. ^1H NMR (500 MHz, CDCl_3): δ_{H} 2.98 (d, 1H, $J = 17.55$ Hz, H-5a), 3.20 (d, 1H, $J = 17.55$ Hz, H-5b), 3.57 (d, 1H, $J = 15.05$ Hz, H-7a), 3.79 (d, 1H, $J = 15.05$ Hz, H-7b), 4.89 (s, 1H, H-4), 6.60 (s, 1H, H-9), 6.97–7.27 (m, 8H, aromatic), 8.00 (s, 1H, NH), 8.09 (s, 1H, NH); ^{13}C NMR (125 MHz, CDCl_3): δ_{C} 45.33, 45.44, 58.53, 112.74, 115.74, 116.03, 116.36, 116.65, 121.61, 126.19, 127.04, 129.24, 127.04, 129.24, 129.35, 131.31, 131.42, 131.88, 131.92, 137.12, 137.17, 160.78, 161.53, 164.07, 164.81, 174.18.

4.2.23. (E)-8-(2,4-Dichlorobenzylidene)-4-(2,4-dichlorophenyl)-3,4,5,6,7,8-hexahydropyrido[4,3-d]pyrimidine-2(1H)-thione (7k)

Yellow solid; mp 136–139 °C; Anal. Calcd for $\text{C}_{20}\text{H}_{15}\text{Cl}_4\text{N}_3\text{S}$ C, 50.98; H, 3.21; N, 8.92. Found: C, 51.55; H, 3.08; N, 8.69. ^1H NMR (500 MHz, CDCl_3): δ_{H} 3.05 (d, 1H, $J = 17.91$ Hz, H-5a), 3.32 (d, 1H, $J = 17.91$ Hz, H-5b), 3.49 (d, 1H, $J = 15.00$ Hz, H-7a), 3.65 (d, 1H, $J = 15.07$ Hz, H-7b), 5.44 (s, 1H, H-4), 6.61 (s, 1H, H-9) 7.02–7.49 (m, 6H, aromatic), 7.74 (s, 1H, NH), 8.12 (s, 1H, NH); δ_{C} 45.21,

45.47, 54.75, 112.56, 119.07, 126.99, 127.34, 128.94, 129.14, 129.99, 130.16, 130.81, 131.87, 132.59, 133.59, 134.74, 135.02, 135.73, 136.64, 174.76.

4.2.24. (E)-4-(Naphthalen-1-yl)-8-(naphthalen-1-ylmethylene)-3,4,5,6,7,8-hexahydropyrido[4,3-d]pyrimidin-2(1H)-thione (71)

Yellow solid; mp 141–143 °C; Anal. Calcd for C₂₈H₂₃N₃S C, 77.57; H, 5.35; N, 9.69. Found: C, 78.29; H, 5.94; N, 8.45; ¹H NMR (500 MHz, CDCl₃): δ_H 3.09 (d, 1H, J = 17.15 Hz, H-5a), 3.19 (d, 1H, J = 17.15 Hz, H-5b), 3.71 (d, 1H, J = 15.07 Hz, H-7a), 3.94 (d, 1H, J = 15.07 Hz, H-7b), 5.49 (s, 1H, H-4), 6.63 (s, 1H, H-9), 6.81–8.17 (m, 16H, H-aromatic, NH); ¹³C NMR (125 MHz, CDCl₃): δ_C 45.71, 45.78, 55.17, 112.34, 122.43, 128.11, 126.75, 127.12, 127.44, 127.98, 129.48, 129.76, 129.96, 133.12, 133.54, 137.17, 138.32, 139.62, 174.49.

4.3. In vitro cholinesterase enzymes inhibitory activity

The test samples for cholinesterase enzymes inhibitory potential was evaluated using modified Ellman's method as described by Ahmed and Gilani.²⁵ Galanthamine was used as positive control. Solutions of test samples and galanthamine were prepared in DMSO at an initial concentration of 1 mg/mL (1000 ppm). The concentration of DMSO in final reaction mixture was 1%. At this concentration, DMSO has no inhibitory effect on both acetylcholinesterase and butyrylcholinesterase enzymes.²⁶

For acetylcholinesterase (AChE) inhibitory assay, 140 μL of 0.1 M sodium phosphate buffer of pH 8 was first added to a 96-wells microplate followed by 20 μL of test samples and 20 μL of 0.09 units/mL acetylcholinesterase enzyme. After 15 min. of incubation at 25 °C, 10 μL of 10 mM 5,5'-dithiobis-2-nitrobenzoic acid (DTNB) was added into each well followed by 10 μL of 14 mM acetylthiocholine iodide. Thirty min after the initiation of enzymatic reaction, absorbance of the colored end-product was measured using BioTek PowerWave X 340 Microplate Spectrophotometer at 412 nm. For butyrylcholinesterase (BChE) inhibitory assay, the same procedure described above was followed, except for the use of enzyme and substrate, instead of which, butyrylcholine esterase from equine serum and S-butrylthiocholine chloride were used.

Each test was conducted in triplicate. Absorbance of the test samples was corrected by subtracting the absorbance of their respective blank. Percentage inhibition was calculated using the following formula:

$$\text{Percent of inhibition} = \frac{\text{Absorbance of control} - \text{Absorbance of Sample}}{\text{Absorbance of control}} \times 100$$

4.4. Molecular modeling study

To date, there are a total of 145 AChE and 29 BChE co-crystal structures and NMR structures available in Protein Data Bank (PDB).²⁷

Using Glide, (version 5.7, Schrödinger, LLC, New York, NY, 2011), most active compounds were docked onto the active site of TcAChE derived from three-dimensional structure of the enzyme complex with anti-Alzheimer's drug, E2020 (Aricept™) (PDB ID: 1EVE) and to BChE derived from complex of the enzyme with Tabun analogue (PDB code: 2W1J).

Water molecules and hetero groups were deleted from receptor beyond the radius of 5 Å of reference ligand (E2020 or Tabun), resulting protein structure refined and minimized by Protein

Preparation Wizard using OPLS-2005 force field. Receptor Grid Generation program were used to prepare AChE and BChE grid and all the ligands were optimized by LigPrep program by using OPLS-2005 force field to generate lowest energy state of respective ligands. Docking stimulations were carried out on bioactive compounds, handed in five poses per ligand, in which the best pose with highest score was displayed for each ligand.

Acknowledgments

We would like to thank the Malaysian Government and Universiti Sains Malaysia (USM) for the Research University Grant (1001/PFARMASI/813031). A.B. is supported by the USM Graduate Assistant Scheme from the Institute for Postgraduate Studies (IPS) of Universiti Sains Malaysia.

Supplementary data

Supplementary data associated with this article can be found, in the online version, at <http://dx.doi.org/10.1016/j.bmc.2013.03.058>.

References and notes

- Batsch, N. L.; Mittelman, M. S. *World Alzheimer Report 2012 Overcoming the stigma of dementia*; Alzheimer's Disease International: London, 2012.
- Hardy, J. J. *Alzheimers Dis.* **2006**, *9*, 151.
- Terry, A. V.; Buccafusco, J. J. *J. Pharmacol. Exp. Ther.* **2003**, *306*, 821.
- Tabet, N. *Age Ageing* **2006**, *35*, 336.
- Giacobini, E. *Pharmacol. Res.* **2004**, *50*, 433.
- Giacobini, E. *Neurochem. Int.* **1998**, *32*, 413.
- Rampa, A.; Piazzi, L.; Belluti, F.; Gobbi, S.; Bisi, A.; Bartolini, M.; Andrisano, V.; Cavrini, V.; Cavalli, A.; Recanatini, M.; Valenti, P. J. *Med. Chem.* **2001**, *44*, 2279.
- Giacobini, E. *Drugs Aging* **2001**, *18*, 891.
- Greig, N. H.; Utsuki, T.; Ingram, D. K.; Wang, Y.; Pepeu, G.; Scali, C.; Yu, Q. S.; Mamczarz, J.; Holloway, H. W. *Proc. Natl. Acad. Sci. U.S.A.* **2005**, *102*, 17213.
- Haroutunian, V.; Greig, N.; Pei, X. F.; Utsuki, T.; Gluck, R.; Acevedo, L. D.; Davis, K. L.; Wallace, W. C. *Mol. Brain Res.* **1997**, *46*, 161.
- Giacobini, E. In *Cholinesterases and Cholinesterase Inhibitors*; Giacobini, E., Ed.; Martin Dunitz: London, 2000; p 181.
- Kitchen, D. B.; Decornez, H.; Furr, J. R.; Bajorath, J. *Nat. Rev. Drug Disc.* **2004**, *3*, 935.
- Koellner, G.; Steiner, T.; Millard, C. B.; Silman, I.; Sussman, J. L. *J. Mol. Biol.* **2002**, *320*, 721.
- Nicolet, Y.; Lockridge, O.; Masson, P.; Fontecilla-Camps, J. C.; Nachon, F. *J. Biol. Chem.* **2003**, *278*, 41141.
- Atwal, K. S.; Rovnyak, G. C.; O'Reilly, B. C.; Schwartz, J. J. *Org. Chem.* **1989**, *54*, 5898.
- Rovnyak, G. C.; Atwal, K. S.; Hedberg, A.; Kimball, S. D.; Moreland, S.; Gougoutas, J. Z.; O'Reilly, B. C.; Schwartz, J.; Malley, M. F. *J. Med. Chem.* **1992**, *35*, 3254.
- Nagarathnam, D.; Miao, S. W.; Lagu, B.; Chiu, G.; Fang, J.; Dhar, T. G. M.; Zhang, J.; Tyagarajan, S.; Marzabadi, M. R.; Zhang, F. *J. Med. Chem.* **1999**, *42*, 4764.
- Kappe, C. O. *Eur. J. Med. Chem.* **2000**, *35*, 1043.
- Black, G. P.; Coles, S. J.; Hizi, A.; Howard-Jones, A. G.; Hursthouse, M. B.; McGown, A. T.; Loya, S.; Moore, C. G.; Murphy, P. J.; Smith, N. K. *Tetrahedron Lett.* **2001**, *42*, 3377.
- Mayer, T. U.; Kapoor, T. M.; Haggarty, S. J.; King, R. W.; Schreiber, S. L.; Mitchison, T. J. *Science* **1999**, *286*, 971.
- Patil, A. D.; Kumar, N. V.; Kokke, W. C.; Bean J. *Org. Chem.* **1995**, *60*, 1182.
- Dimmock, J. R.; Padmanilayam, M. P.; Puthucode, R. N.; Nazarali, A. J.; Motaganahalli, N. L.; Zello, G. A.; Quail, J. W.; Oloo, E. O.; Kraatz, H. B.; Prisciak, J. S. *J. Med. Chem.* **2001**, *44*, 586.
- Guillozet, A.; Smiley, J. F.; Mash, D. C.; Mesulam, M. M. *Ann. Neurol.* **1997**, *42*, 909.
- Wong, K. K. K.; Ngo, J. C. K.; Liu, S.; Lin, H.; Hu, C.; Shaw, P. C.; Wan, D. C. C. *Chem. Biol. Interact.* **2010**, *187*, 335.
- Ahmed, T.; Gilani, A. H. *Pharmacol. Biochem. Behav.* **2009**, *91*, 554.
- Obregon, A.; Schetinger, M.; Correa, M. M.; Morsch, V. M.; Da Silva, J.; Martins, M.; Bonaccorso, H. G.; Zanatta, N. *Neurochem. Res.* **2005**, *30*, 379.
- Berman, H. M.; Westbrook, J.; Feng, Z.; Gilliland, G.; Bhat, T. N.; Weissig, H.; Shindyalov, I. N.; Bourne, P. E. *Nucleic Acids Res.* **2000**, *28*, 235.
- Kreienkamp, H. J.; Weise, C.; Raba, R.; Aaviksaar, A.; Hucho, F. *Proc. Natl. Acad. Sci. U.S.A.* **1991**, *88*, 6117.
- Silman, I.; Sussman, J. L. *Chem. Biol. Interact.* **2008**, *175*, 3.